

The BiomolBiomed publishes an “Advanced Online” manuscript format as a free service to authors in order to expedite the dissemination of scientific findings to the research community as soon as possible after acceptance following peer review and corresponding modification (where appropriate). An “Advanced Online” manuscript is published online prior to copyediting, formatting for publication and author proofreading, but is nonetheless fully citable through its Digital Object Identifier (doi®). Nevertheless, this “Advanced Online” version is NOT the final version of the manuscript. When the final version of this paper is published within a definitive issue of the journal with copyediting, full pagination, etc., the new final version will be accessible through the same doi and this “Advanced Online” version of the paper will disappear.

RESEARCH ARTICLE

Wang et al: TMGs in CRC prognosis

Role of telomere maintenance genes as a predictive biomarker for colorectal cancer immunotherapy response and prognosis

Zhikai Wang^{1#}, Chunyan Zhao^{2#}, Yifen Huang^{3*}, Chong Li^{2*}

¹Department of Gastrointestinal Surgery, Henan Provincial People's Hospital, Zhengzhou, China

²Department of Oncology, The Affiliated Dazu's Hospital of Chongqing Medical University, Chongqing, China

³Outpatient Department, The Affiliated Dazu's Hospital of Chongqing Medical University, Chongqing, China

*Correspondence to **Yifen Huan**: 3516882473@qq.com and **Chong Li**: 152389@hospital.cqmu.edu.cn

[#]Equally contributed to this work: **Zhikai Wang** and **Chunyan Zhao**

DOI: <https://doi.org/10.17305/bb.2025.12053>

ABSTRACT

Colorectal cancer (CRC) represents a significant global health challenge. Although telomere maintenance plays a crucial role in tumorigenesis, the prognostic value and immunotherapeutic relevance of telomere maintenance genes (TMGs) in CRC remain poorly understood. In this study, relevant data were retrieved from The Cancer Genome Atlas (TCGA) and the Gene Expression Omnibus (GEO) databases. TMG scores were calculated using the single-sample gene set enrichment analysis (ssGSEA) method, and TMGs associated with prognosis were subsequently identified. TCGA-CRC samples were classified into subtypes via consensus clustering (ConsensusClusterPlus). A risk prediction model was then constructed using univariate and Lasso Cox regression analyses. Survival analysis was performed using Kaplan–Meier curves generated with the survival package. Key genes were validated *in vitro* using cellular models. Immune cell infiltration was evaluated through ssGSEA, TIMER, and MCP-Counter tools, and chemotherapy responses were predicted using the pRRophetic package. From 28 prognosis-related TMGs, two distinct CRC subtypes were established, with subtype C1 demonstrating more favorable clinical outcomes. Additionally, a risk model incorporating seven TMG-related genes (CDC25C, CXCL1, RTL8C, FABP4, ITLN1, MUC12, and ERI1) was developed for CRC prognosis. Differential mRNA expression levels of these genes were confirmed between CRC cell lines and normal control cells. Furthermore, silencing MUC12 suppressed CRC cell migration and invasion *in vitro*. Importantly, CRC patients classified as low-risk exhibited superior responses to immunotherapy, whereas high-risk patients showed increased sensitivity to conventional anti-cancer treatments. This study represents the first systematic evaluation of TMGs in CRC prognosis and immunotherapy, providing novel insights that could inform personalized therapeutic strategies.

Keywords: Immunotherapy; Risk model; Prognostic signature; Telomere maintenance gene; Colorectal cancer.

INTRODUCTION

Colorectal cancer (CRC) ranks among the most prevalent malignancies of the digestive system [1, 2], with projections suggesting it will affect approximately 2.5 million individuals by 2035 [3]. Globally, CRC accounts for 9.6% of all cancer cases, making it the third most frequently diagnosed cancer [4]. It is also the second leading cause of cancer-related death, responsible for 9.3% of deaths, which translates to approximately 900,000 deaths worldwide each year [4, 5]. Due to its asymptomatic nature in the early stages, timely diagnosis and treatment remain challenging, underscoring the need for more advanced screening methods [6, 7]. While studies have identified transcription factors (e.g., Nrf2) and ferroptosis-related genes (such as GSH, GPX4, and P53) as potential therapeutic targets for CRC [8], the lack of reliable biomarkers continues to hinder the accuracy of prognostic predictions [9]. Therefore, identifying biomarkers specific to CRC and developing robust prognostic models are crucial for the early detection and prognosis of the disease [10]. Telomeres, which consist of protective proteins and TTAGGG repeats [11, 12], are nucleoprotein complexes located at the ends of human chromosomes. Studies have shown that telomeres play essential roles in maintaining chromosomal and genomic stability [13]. However, during certain cell divisions or disease states, telomere length gradually shortens [14, 15]. To maintain their length, telomerase adds TTAGGG sequences to the chromosomal ends [16, 17]. Increasing evidence links the shortening of telomere length to the development of various diseases, including tumors [13, 18, 19]. It has been observed that telomere maintenance genes (TMGs) influence cancer occurrence by regulating mutations in the telomerase reverse transcriptase (TERT) promoter, suggesting their potential as cancer biomarkers [20, 21]. Two mechanisms for telomere elongation [22] have been identified in cancers: telomerase activation [23] and alternative lengthening of telomeres (ALT) [24]. Telomerase overexpression is commonly observed in many tumor cells [25, 26], while abnormal activation of ALT has been detected in telomerase-negative tumors, such as those in thyroid cancer [27]. Despite these findings, the prognostic value of TMGs in CRC remains unclear and warrants further investigation to enhance current therapeutic strategies. This study was designed to systematically evaluate the expression patterns, molecular subtypes, and prognostic significance of TMGs in CRC, along with their interactions with the immune microenvironment and correlations with treatment responses. Using

transcriptomic data from public CRC databases, the ssGSEA method was employed to compute TMG expression scores, and key survival-related genes were identified. Molecular subtypes were classified based on prognostically correlated TMGs using a consensus clustering method. Differential expression and functional enrichment analyses were then performed to explore the potential biological mechanisms. A RiskScore model was developed to assess the performance of TMGs in evaluating immune cell infiltration, immunotherapy response, chemotherapy sensitivity, and survival outcomes in CRC patients. Finally, *in vitro* experiments were conducted to validate the expression and biological functions of key genes. Collectively, our findings highlight the critical role of TMGs in immune regulation and CRC development, providing new insights for personalized treatment and risk assessment.

MATERIAL AND METHODS

Acquisition and preprocessing of data

CRC data, including clinical information for both colon and rectum adenocarcinomas, copy number variations (CNVs), and somatic mutations, were retrieved from the TCGA database (<https://portal.gdc.cancer.gov/>). After excluding samples without survival data, 589 tumor samples with survival times greater than 0 days were retained. The RNA-seq expression profiles were converted to TPM format and log2-transformed. Additionally, we downloaded GSE17537 microarray data from GEO (<https://www.ncbi.nlm.nih.gov/geo>) and converted the probes to gene symbols based on the annotation file. After excluding samples without clinical follow-up or survival data, 55 tumor samples from GSE17537 were retained. Finally, 2093 TMGs were extracted from a previous study [28].

Identification of CRC-related TMGs and analysis of their mutations and CNVs

Using the ssGSEA method, TMG scores for the TCGA-CRC dataset were computed. DEGs between tumor and adjacent tissues were identified and intersected with TMG signatures. Prognosis-correlated TMGs were then selected through univariate Cox regression analysis. CNV and mutation data from the TCGA database were collected. Briefly, MuTect2 [29] was used to analyze the mutational landscape of TMG in primary CRC samples from the TCGA-CRC cohort, followed by visualization of the mutational status in a waterfall plot with the maftools R package [30]. The CNV status of the TMGs in primary CRC samples was then

assessed using ADTEx [31].

Molecular clustering

Consensus clustering was performed on the tumor samples using the ConsensusClusterPlus package [32], with hierarchical clustering (clusterAlg = "hc") and Pearson correlation distance (distance = "pearson") as the clustering parameters. The analysis was conducted over 500 iterations with a resampling rate of 80%. The optimal number of clusters (k) was determined based on the stabilized cumulative distribution function (CDF) curve, minimal incremental gains in the delta area plots, and high intra-cluster consensus with clear inter-cluster separation in the consensus matrices. Finally, the clinical features (M.stage, N.stage, T.stage, stage, status, age, and gender) and prognosis across the different molecular subtypes were systematically assessed.

Enrichment analysis

DEGs between C1 and C2 were identified using the limma package (false discovery rate < 0.05 & |log2FC| > log2(1.5)) [33] to select common genes for enrichment analysis. The TCGA-CRC cohort was then subdivided into two molecular subtypes based on the DEGs. Next, the clusterProfiler R package [34] was used to conduct GO and KEGG enrichment analysis [35].

Establishment of a risk model

The prognosis-correlated DEGs were screened using univariate Cox regression analysis, followed by refinement of the risk model with Lasso Cox regression from the glmnet package [36] and 10-fold cross-validation. A RiskScore model was then formulated through stepwise multivariate Cox regression analysis as follows:

$$\text{RiskScore} = \sum \beta_i \times \text{Exp}_i$$

Where β_i represents the coefficient of a gene in the Cox regression model, and Exp_i represents the gene expression. The samples were divided into low- and high-risk groups based on the median RiskScore as the threshold. Survival differences between the two groups were then analyzed using Kaplan-Meier (KM) curves with the survival package [37]. The prognostic classification of the RiskScore model was validated through receiver operating characteristic

(ROC) analysis using the timeROC R package [38] and principal component analysis (PCA). Additionally, the prognostic differences between the two risk groups across gender, age, and stage were compared by calculating the RiskScores for all patients.

Independent clinical and pathological factors (stage, M.stage, N.stage, T.stage, status, age, and gender) for CRC prognosis were selected using univariate and multivariate Cox regression analyses, along with the RiskScore model. To predict 1-, 3-, and 5-year survival for CRC patients, a prognostic nomogram was developed using the rms package [39]. Finally, the clinical reliability of the nomogram was assessed by calibration curve analysis and decision curve analysis (DCA).

Tumor microenvironment (TME) differences across the risk groups

Immune cell infiltration in each risk groups was comprehensively examined using the ssGSEA algorithm, the MCPcounter package [40], and the TIMER online tool (<http://cistrome.org/TIMER>). Specifically, the TIMER offer six main analysis modules to enable the correlation analysis between a range of factors and immune infiltration.

Culture and transfection of cells

Human colon adenocarcinoma cells (SW1116, BNCC100262) and normal human colon epithelial cells (NCM460, BNCC339288), both obtained from the BeiNa Culture Collection (Beijing, China), were cultured in either RPMI Medium 1640 (31800, Solarbio Lifesciences, Beijing, China) or Leibovitz's L-15 Cell Culture Medium (LA9510, Solarbio Lifesciences). Both media were supplemented with 10% FBS (S9020, Solarbio Lifesciences). The cultures were maintained at 37°C to ensure optimal growth conditions. For NCM460 cells, the culture was performed in an incubator with 5% CO₂. The siRNA was synthesized by GenePharma (Suzhou, China) and transfected into MUC12 cells using Lipofectamine 2000 (11668027, Invitrogen, Carlsbad, CA). The negative control, which contained a scrambled target sequence (5'-ACCAGTATTGGAGGTAATACAAC-3'), was purchased [41].

Wound healing assay

A controlled artificial wound was created on the cell monolayers using a 10 µL pipette tip after culturing the transfected CRC cells SW1116 (1×10^5 cells/well) to full confluence in a 6-well

plate. The cells were then cultured in serum-free medium at 37°C. Photographs were taken at 0 hours (h) and 48 hours (h) using an Eclipse Ts2R microscope (Nikon, Tokyo, Japan).

Transwell assay

Matrigel (50 µL, Corning, Inc.) was used to pre-coat the transwell chambers (pore size: 8 µm, 3422, Corning, Inc., Corning, NY), which were placed on 24-well plates. Next, the transfected SW1116 cells in serum-free medium (200µL) were planted into the upper chamber at 1×10^5 cells/well, whereas the lower transwell chamber contained 700 µL complete medium. After cell culture for 48 h, the cells were fixed by 4% paraformaldehyde (P1110, Solarbio Lifesciences) for 30 minutes (min), followed by using 0.1% crystal violet solution (G1063, Solarbio Lifesciences) for cell staining another 15 min. Finally, the cells were observed and quantified under the microscope used in the previous assay.

QRT-PCR analysis

Total RNA was extracted from NCM460 and SW1116 cells using the TriZol kit (15596026CN, Invitrogen) and then reverse transcribed into cDNA with a first-strand cDNA synthesis kit (1708890, Bio-Rad Laboratories, Hercules, CA). Quantitative PCR (qPCR) amplification was performed using a CFX384 qPCR System (1855484, Bio-Rad Laboratories) with SYBR Green Supermix (1708880, Bio-Rad Laboratories), under the following cycling conditions: initial denaturation at 95°C for 2 minutes, followed by 40 cycles of denaturation at 95°C for 15 seconds, annealing at 60°C for 30 seconds, and extension at 72°C for 30 seconds. GAPDH was used as the normalization control, and relative mRNA expression was calculated using the $2^{-\Delta\Delta C}$ method [42]. Primers are listed in Table S1.

Immunotherapy and drug sensitivity

Immunotherapy responses were predicted by standardizing the transcriptome data applying TIDE (<http://tide.dfci.harvard.edu/>) to calculate the TIDE scores, with higher TIDE scores showing greater possibility of immune escape and less immunotherapy benefit. Next, chemotherapy sensitivity in the TCGA-CRC dataset and the differences of patients' responses were analyzed and compared by the pRRophetic software package [43]. Patients' sensitivity in different risk groups to chemotherapy agents was evaluated with IC50.

Statistical analysis

All analyses were conducted using R (version 3.6.0). The normality of data distribution was assessed with the Shapiro-Wilk test prior to testing for variance. For comparisons between two independent groups of continuous variables, the Wilcoxon rank-sum test was applied. The Kruskal-Wallis test was used to examine differences in continuous variables among three groups. The Chi-square test was employed to assess disparities in categorical variables across different groups. Additionally, the log-rank test was used to compare survival times between patients in different groups. $P < 0.05$ denoted a statistical significance. For *in vitro* cellular experiments, differences between the normal and experimental groups were analyzed using Student's t-test with GraphPad Prism 8.0 software. Data are presented as the mean \pm standard deviation (SD). Analytical support for this study was provided by SangerBox (<http://sangerbox.com/>) [44].

RESULTS

Genomic landscape of the TMGs in CRC

Using ssGSEA analysis, we first computed the TMG scores in the TCGA-CRC dataset. The results showed that tumor tissues exhibited significantly higher TMG scores than adjacent non-tumor tissues (Figure 1A). Further analysis identified 317 DEGs between the two tissue types (Figure 1B), among which 28 TMGs were found to have significant prognostic relevance in CRC based on univariate Cox regression analysis (Figure 1C). Additionally, an analysis of the mutational status and CNVs of these 28 TMGs in the tumor samples revealed that only 23.69% of the samples carried gene mutations associated with telomere maintenance (Figure 1D). Among these, *SNAIL* and *RBL1* showed relatively higher frequencies of copy number amplification (Figure 1E).

Identification of CRC molecular subtypes based on TMGs

In this study, we use consistency clustering to analyze TCGA-CRC samples, utilizing a combination of CDF curves, Delta Area plots, and consistency matrix heatmaps. The stability and reasonableness of different clustering numbers (k) are evaluated by examining these plots. First, the CDF curves (Figure 2A) show that as the number of clusters increases from $k=2$ to $k=3$, the curves shift toward the upper right corner, indicating improved clustering consistency. However, the improvement is significantly smaller after $k=3$. Figure 2B further demonstrates

that the largest increment in CDF area occurs between $k=2$ and $k=3$, with diminishing returns at $k \geq 4$, suggesting limited benefits to increasing the number of clusters beyond $k=3$. Additionally, Figure 2C shows that with $k=2$, the heatmap reveals high consistency within clusters, clear separation between clusters, and a robust clustering structure. Based on these analyses, we determined that $k=2$ is the optimal number of clusters, dividing the samples into two groups: C1 and C2. Survival analysis indicated significantly better overall survival in C1 compared to C2 (Figure 2D, $P = 0.0015$). Clinical feature analysis revealed differences in M.stage and status between the two subtypes. Comparison of TMG expression profiles showed that C1 had higher expression levels of multiple genes, including RBL1, CHEK1, BRCA1, HMMR, KPNA2, CCNA2, NCAPG, TKT, TRAP1, ORC1, CDC45, CCT2, and CCNB1 (Figure 2E). These findings confirm the robust classification of CRC samples into two molecular subtypes with significant survival differences and clinical heterogeneity, providing a strong foundation for future molecular subtyping studies.

Enrichment analysis results of the DEGs

Differential expression analysis using limma package [45] identified 538 DEGs between C1 and C2 (282 upregulated in C1, 256 upregulated in C2). GO and KEGG enrichment analysis showed that C1-associated genes were mainly enriched in proliferation-related pathways including DNA replication and cell cycle (**Figure. 3A-D**), while C2-associated genes were mainly enriched in pathways related to cancer metastasis and invasion such as focal adhesion, extracellular matrix organization, extracellular matrix (ECM)-receptor interaction (**Figure. 3E-H**). These results demonstrated significant differences between the two subtypes in terms of potential therapeutic response and biological behaviors in CRC.

Development of a risk model based using the seven TMGs

Through univariate Cox analysis, we identified 101 prognostic DEGs ($P < 0.05$), which were finally refined to seven key genes (*CDC25C*, *CXCL1*, *RTL8C*, *FABP4*, *ITLN1*, *MUC12*, and *ERII*) by Lasso Cox regression analysis with 10-fold cross-validation (Figure. 4A) and stepwise multivariate Cox regression analysis (**Figure. 4B**). The formula of the RiskScore model was as follow:

$$\text{RiskScore} = (0.155 * \text{RTL8C}) + (0.080 * \text{FABP4}) + (-0.062 * \text{ITLN1}) +$$

$(-0.100 * CXCL1) + (-0.122 * MUC12) + (-0.282 * ERI1) + (-0.285 * CDC25C)$. Patients were allocated by the median value of RiskScore into low-risk and high-risk groups. KM survival curve demonstrated that the two risk groups in the TCGA-CRC training cohort differed significantly in patients' survival, with those having a higher RiskScore showing shorter overall survival (OS) (**Figure. 4C**). The timeROC package [38] was employed in ROC analysis for further validating the prognosis classification of the RiskScore. The AUC values in the training dataset for 1-, 3-, and 5-year survival were 0.63, 0.68, and 0.72, respectively, which suggested a highly accurate survival evaluation by the model (**Figure. 4C**). Furthermore, PCA results also showed a distinct separation between the two risk groups in the TCGA-CRC cohort (**Figure. 4D**), further supporting the performance of the RiskScore in identifying CRC patients with different risks.

The robustness of the RiskScore was confirmed using the validation dataset GSE17537 (Figures 4E-F). Consistently, the RiskScore value showed a negative correlation with survival outcomes in this dataset. A comparison of the performance between the low- and high-risk groups across different clinical factor subgroups revealed significant differences ($P < 0.05$), independent of stage classification (I + II vs. III + IV), gender (male vs. female), or age (> 67 or ≤ 67). This suggests that the RiskScore provides an independent risk classification, less likely to be influenced by other clinical factors (Figures 4G-I).

Validation of the TMG-related risk model

Analysis of the TCGA cohort revealed strong associations between risk groups and pathological staging, with the high-risk group showing a higher prevalence of the C2 subtype and metastasis cases. This finding aligns with our previous research, which demonstrated that the C2 cluster is enriched in metastasis-related pathways. Further analysis indicated that the RiskScore correlated positively with more advanced clinical stages (T.stage, N.stage, and overall stage). Figures 5A and 5B illustrate the relationship between clinical features and RiskScore, along with a violin plot, respectively. Both univariate and multivariate Cox regression analyses identified M.stage, stage, RiskScore, and age as significant prognostic factors for CRC (Figures 5C-D). A nomogram was developed by integrating other clinical and pathological characteristics with the RiskScore to estimate survival and risk for CRC patients

(Figure 5E). The results highlighted the RiskScore as the most influential factor for survival prediction. Calibration curves revealed that the 1-, 3-, and 5-year prediction curves closely aligned with the reference curve (Figure 5F), indicating strong predictive performance of the nomogram. Additionally, Decision Curve Analysis (DCA) demonstrated superior clinical effectiveness and reliability of the nomogram (Figure 5G).

***In vitro* verification of the key genes for CRC prognosis**

The relative expressions of the seven genes (*CDC25C*, *CXCL1*, *RTL8C*, *FABP4*, *ITLN1*, *MUC12*, and *ERII*) in SW1116 and NCM460 cells were measured. It was found that the expressions of *ITLN1* and *ERII* were notably downregulated in SW1116 cells, while the mRNA expressions of *CDC25C*, *CXCL1*, *RTL8C*, *FABP4*, and *MUC12* were significantly higher in SW1116 cells than in control NCM460 cells (**Figure. 6A-G**, $P < 0.05$).

Previous study found the potential of *MUC12* as a molecular marker for the prognosis of CRC [46, 47]. Therefore, this study performed wound healing and transwell assays to evaluate the potential effects of *MUC12* knockdown on CRC cells. As shown in **Figure. 6H-I**, *MUC12* knockdown notably suppressed the migration and invasion abilities of SW1116 cells ($P < 0.01$). This result was consistent with the cancer-promoting role of *MUC12*, which further supported the clinical significance of the RiskScore model developed based on TMGs.

Differences in the TME between CRC patients with different risks

The ssGSEA analysis showed that the infiltration of Type 17 T helper cells, neutrophils, activated B cells, Type 2 T helper cells, activated CD4 T cells, and activated CD8 T cells—immune cells typically involved in killing tumor cells [48]—was lower in the high-risk group compared to the low-risk group. This reduced infiltration may contribute to the protection of tumor cells. Additionally, regulatory T cells, which are highly expressed in the high-risk group, could promote tumor development (Figure 7A). TIMER analysis further revealed that CD8⁺ T cells and B cells were less expressed in the high-risk group (Figure 7B). MCPcounter analysis (Figure 7C) identified significant differences in the infiltration of several cell types between the two groups. Specifically, the high-risk group exhibited significantly lower infiltration of NK cells, cytotoxic lymphocytes, T cells, neutrophils, and B lineage cells. These findings suggest that the absence of immune effector cells may contribute to a "cold-immune" tumor

microenvironment (TME) in high-risk patients, which could explain their poorer prognosis.

Immunotherapy and drug sensitivity analysis for CRC patients in different risk groups

TIDE analysis revealed significantly lower TIDE scores in the low-risk group (**Figure. 8A**), suggesting more active immune response and less immune evasion possibility in those patients. Further analysis showed that the low-risk group had a significantly higher expression level of the immune checkpoint inhibitor CD274 (PD-L1) than the high-risk group (**Figure. 8B**), indicating a better response of low-risk patients to immune checkpoint blockade therapy. Based on the ssGSEA algorithm and an established gene signature [49], the responsiveness to treatments including anticancer immunotherapy and chemotherapy was analyzed. It was observed that low-risk CRC patients had a higher reactivity across multiple treatment-correlated gene sets (**Figure. 8C-E**), while high-risk CRC patients had higher sensitivities to common anti-cancer drugs, for instance, Phenformin, MG.132, Cyclophosphamide, and Sorafenib (**Figure. 8F**). These findings highlighted that patients in different risk groups responded differently to the therapeutic strategies, with low-risk patients benefiting more from immunotherapy and high-risk patients benefiting more from conventional anti-tumor drug treatments.

DISCUSSION

CRC diagnosis remains challenging due to its asymptomatic nature in the early stages, which results in a poor prognosis. This underscores the need for effective prognostic biomarkers to reduce the mortality rate in CRC patients [7]. Telomere length in lymphocytes is closely linked to tumor development, and telomere shortening is considered a prognostic marker for CRC [50]. While genes like RCN3 have emerged as potential prognostic markers, their specific mechanisms still require further investigation [51]. Therefore, this study developed a novel TMG-based risk model for prognostic assessment in CRC to contribute to the field. Clustering analysis identified two distinct CRC subtypes (C1, C2) based on TCGA-CRC samples, with the C2 subtype exhibiting higher copy number and expression of SNAIL and a poorer prognosis. SNAIL has been found to play a pivotal role in maintaining telomere integrity [52], and its absence promotes telomerase activity in mesenchymal stem cells, highlighting the potential of

SNAIL as a crucial TMG in this process [52]. SNAIL also regulates epithelial-mesenchymal transition (EMT) [53], a process during which epithelial cells lose their connections and polarity but acquire mesenchymal properties and invasive abilities [54]. Such phenotypic changes during EMT contribute to tumorigenesis. The expression level and function of SNAIL have been widely studied in many types of cancer, including CRC. SNAIL drives stem cell properties, metabolic alterations, cancer invasion, and chemoresistance in epithelial ovarian cancer [55], promotes metastasis in breast tumors [56], and high expression of SNAIL is considered a clinical biomarker in gastric cancer [57]. In CRC, intestinal epithelial SNAIL facilitates tumor development through EMT and the Wnt/ β -catenin signaling pathway [58]. Furthermore, studies on both CRC patients and *in vitro* experiments have shown that SNAIL expression predicts patient response to drug treatment [59]. This study found that SNAIL had a higher CNV, consistent with previous findings that CNVs frequently occur in regions containing genes crucial for CRC, making them potential biomarkers for cancer detection [60]. Thus, this study proposed SNAIL as a promising candidate for early CRC detection. Recent studies highlight the multifaceted roles of the seven identified TMGs (CDC25C, CXCL1, RTL8C, FABP4, ITLN1, MUC12, and ERI1) in carcinogenesis. For instance, CDC25C plays a critical role in regulating the G2/M phase of the cell cycle, and its expression changes are implicated in cancer growth [61]. CXCL1, a member of the CXC chemokine subfamily, demonstrates clinical significance in various cancer types [62]. FABP4, abundant in adipocytes, is upregulated in multiple solid tumors, indicating a poor prognosis [63]. RTL8C has potential as a promising pan-cancer biomarker [64]. High expression of ERI1 is linked to improved overall survival in CRC [65]. ITLN, primarily generated by stromal vascular fraction cells, plays a crucial role in cancer growth [66]. MUC12 is a type of transmembrane mucin typically expressed in the normal colon but less so in the pancreas. Studies have reported lower MUC12 mRNA levels in certain CRC tissues compared to normal colonic tissues [67, 68]. Notably, MUC12 exhibited functional complexity in this study. On one hand, multivariate Cox regression analysis revealed that MUC12 acts as an independent protective prognostic factor, with higher expression associated with longer overall survival. On the other hand, *in vitro* experiments showed that downregulation of MUC12 significantly suppressed CRC cell migration and invasion, suggesting a metastasis-promoting effect. The discrepancy between

"statistically protective" and "functionally pro-carcinogenic" roles potentially indicates a dual function of MUC12 in different pathological stages or microenvironmental contexts. In early stages, MUC12 may play a protective role by maintaining epithelial barrier function, while its overexpression may contribute to EMT and microenvironmental remodeling, promoting tumor cell metastasis and invasion during tumor progression [69, 70]. These findings suggest that the specific role of MUC12 requires further elucidation through more *in vivo* mechanistic studies. For cancer pathogenesis, the tumor microenvironment (TME) is a crucial factor, and its compositional changes can provide insights into patient responses to immunotherapy [71, 72]. In the present study, the high-risk CRC group showed a poorer prognostic outcome, which was consistent with its enrichment in the C2 cluster. We observed that the pathways enriched in C2 were primarily linked to cancer metastasis, suggesting that the worse prognosis in high-risk patients may be attributed to metastasis. High-risk patients also exhibited suppressed immune defense capabilities, leading to an upregulation of immune cell expression. In contrast, low-risk patients demonstrated a more robust immune response. Additionally, the high-risk group showed higher infiltration of endothelial cells and fibroblasts. Endothelial cells are key players in angiogenesis within cancerous tumors [59], a vital process that supplies oxygen and nutrients to tumors [73]. Fibroblasts, a type of mesenchymal cell, are involved in tissue homeostasis and disease processes [74]. The varying infiltration of different immune cell types within the TME may explain the distinctions between the two risk groups. The synergistic effects of fibroblasts and endothelial cells could contribute to tumor metastasis and spread, leading to a worse prognosis for high-risk CRC patients. Interestingly, high-risk patients exhibited an immune system that appeared "suppressed," but they showed greater sensitivity to conventional anti-tumor agents. This suggests that in patients with significant immunosuppression, small molecule targeted therapies might be prioritized over immunotherapy alone. There are several limitations in this study that should be acknowledged. First, while we utilized clinical data and large-scale RNA-seq data from public databases, potential biases could arise from inter-sample heterogeneity, differences in sequencing platforms, and incomplete clinical annotations. These factors may affect the generalizability of our model. Future multicenter prospective studies with larger, independent cohorts are needed to validate and enhance the clinical applicability and robustness of our risk model. Second, while we observed significant differences in immune

cell infiltration and immune checkpoint expression between the two risk groups, the precise molecular mechanisms by which TMGs modulate the TME or contribute to immune evasion remain unclear. Future investigations should integrate single-cell transcriptomics, multi-omics approaches, and functional experiments to systematically explore the immunoregulatory roles of key TMGs and their potential as targets for combination immunotherapy. Lastly, our *in vitro* validation primarily focused on expression profiling, with limited functional characterization. Therefore, more comprehensive studies involving gene knockout or overexpression, as well as animal models, are necessary to strengthen the mechanistic evidence supporting our findings.

CONCLUSION

This study is the first to systematically identify TMGs closely linked to the prognosis of CRC at the whole-genome level and to construct a CRC prognostic risk model consisting of seven key TMGs (CDC25C, CXCL1, RTL8C, FABP4, ITLN1, MUC12, and ERI1). The model demonstrated strong predictive ability across multiple independent cohorts and was also effective in identifying differences in the immune microenvironment and drug sensitivity of CRC patients. Our findings suggest that TMGs influence clinical outcomes in CRC patients by modulating tumor immune escape mechanisms. Combined with *in vitro* experiments, the expression of these key genes was found to be closely related to the invasive ability of CRC cells, further enhancing the biological relevance of the model. This study innovatively integrates the telomere maintenance mechanism with the potential for immunotherapy, providing candidate targets and a novel theoretical foundation for the management and development of targeted therapies for CRC.

Conflicts of interest: Authors declare no conflicts of interest.

Funding: The study was supported by Chongqing Natural Science Foundation General Project (CSTB2023NSCQ-MSX0502) and Chongqing Dazu District Science and Technology Development Project (DZKJ2022JSYJ-KWXM1003).

Data availability: The datasets generated and/or analyzed during the current study are available in the [GSE17537] repository,

[[https://www.ncbi.nlm.nih.gov/geo/query/acc.cgi?acc= GSE17537](https://www.ncbi.nlm.nih.gov/geo/query/acc.cgi?acc=GSE17537)].

Submitted: 14 January, 2025

Accepted: 22 May, 2025

Published online: 02 July, 2025

REFERENCES

1. Li JX, Han T, Wang X, Wang YC, Chen X, Chen WS, et al. Identification of prognostic immune-related lncRNA signature predicting the overall survival for colorectal cancer. *Scientific Reports*. 2023;13(1):1333.
2. Ruan Y, Lu G, Yu Y, Luo Y, Wu H, Shen Y, et al. PF-04449913 Inhibits Proliferation and Metastasis of Colorectal Cancer Cells by Down-regulating MMP9 Expression through the ERK/p65 Pathway. *Current Molecular Pharmacology*. 2023;17.
3. Sharma P, Bora K, Kasugai K, Balabantaray B-K. Two Stage Classification with CNN for Colorectal Cancer Detection. *Oncologie*. 2020;22(3):129--45.
4. Bray F, Laversanne M, Sung H, Ferlay J, Siegel RL, Soerjomataram I, et al. Global cancer statistics 2022: GLOBOCAN estimates of incidence and mortality worldwide for 36 cancers in 185 countries. *CA: a cancer journal for clinicians*. 2024;74(3):229-63.
5. Shi X, Wang Y, Li C, Fu W, Zhang X, Gong A. Knockdown of RCN1 contributes to the apoptosis of colorectal cancer via regulating IP3R1. *Biocell*. 2024;48(5):835-45.
6. Malki A, ElRuz RA, Gupta I, Allouch A, Vranic S, Al Moustafa A-E. Molecular Mechanisms of Colon Cancer Progression and Metastasis: Recent Insights and Advancements. *International Journal of Molecular Sciences*. 2021;22(1):130.
7. Dekker E, Tanis PJ, Vleugels JL, Kasi PM, Wallace MB. Colorectal cancer. *The Lancet Diabetes Endocrinology*. 2019;394(10207):1467-80.
8. Wang Y, Zhang Z, Sun W, Zhang J, Xu Q, Zhou X, et al. Ferroptosis in colorectal cancer: Potential mechanisms and effective therapeutic targets. *Biomedicine & Pharmacotherapy*. 2022;153:113524.
9. Duan L, Yang W, Wang X, Zhou W, Zhang Y, Liu J, et al. Advances in prognostic markers for colorectal cancer*. *Expert Review of Molecular Diagnostics*. 2019;19(4):313-24.
10. Cherri S, Oneda E, Zanotti L, Zaniboni A. Optimizing the first-line treatment for metastatic colorectal cancer. *Frontiers in Oncology*. 2023;13:1246716.
11. Makarov VL, Hirose Y, Langmore JP. Long G tails at both ends of human chromosomes suggest a C strand degradation mechanism for telomere shortening. *Cellular and Molecular Life Sciences*. 1997;88(5):657-66.
12. Brabletz T, Kalluri R, Nieto MA, Weinberg RA. EMT in cancer. *Nature Reviews Cancer*. 2018;18(2):128-34.
13. Nassour J, Schmidt TT, Karlseder J. Telomeres and cancer: resolving the paradox. *Annual Review of Cancer Biology*. 2021;5:59-77.
14. Alder JK, Armanios M. Telomere-mediated lung disease. *Physiological Reviews*. 2022.
15. Brandt M, Dörschmann H, Khraisat Sa, Knopp T, Ringen J, Kalinovic S, et al. Telomere shortening in hypertensive heart disease depends on oxidative DNA damage and predicts impaired recovery of cardiac

function in heart failure. *Hypertension*. 2022;79(10):2173-84.

16. Kim NW, Piatyszek MA, Prowse KR, Harley CB, West MD, Ho PL, et al. Specific association of human telomerase activity with immortal cells and cancer. *Science*. 1994;266(5193):2011-5.
17. Wang F, Tang ML, Zeng ZX, Wu RY, Xue Y, Hao YH, et al. Telomere-and telomerase-interacting protein that unfolds telomere G-quadruplex and promotes telomere extension in mammalian cells. *Proceedings of the National Academy of Sciences*. 2012;109(50):20413-8.
18. in der Stroth L, Tharehalli U, Guenes C, Lechel A. Telomeres and telomerase in the development of liver cancer. *Cancers*. 2020;12(8):2048.
19. Savage SA. Telomere length and cancer risk: finding Goldilocks. *Biogerontology*. 2024;25(2):265-78.
20. Xiao Y, Xu D, Jiang C, Huili Y, Nie S, Zhu H, et al. Telomere maintenance-related genes are important for survival prediction and subtype identification in bladder cancer. *Frontiers in Genetics*. 2023;13.
21. Günes C, Wezel F, Southgate J, Bolenz C. Implications of TERT promoter mutations and telomerase activity in urothelial carcinogenesis. *Nature Reviews Urology*. 2018;15(6):386-93.
22. Liu X, Wang J, Su D, Wang Q, Li M, Zuo Z, et al. Development and validation of a glioma prognostic model based on telomere-related genes and immune infiltration analysis. *Translational cancer research*. 2024;13(7):3182-99.
23. Shay JW, Wright WE. Role of telomeres and telomerase in cancer. *Seminars in Cancer Biology*. 2011;21(6):349-53.
24. Bryan TM, Englezou A, Dalla-Pozza L, Dunham MA, Reddel RR. Evidence for an alternative mechanism for maintaining telomere length in human tumors and tumor-derived cell lines. *Nature Medicine*. 1997;3(11):1271-4.
25. Heidenreich B, Kumar R. TERT promoter mutations in telomere biology. *Mutation Research/Reviews in Mutation Research*. 2017;771:15-31.
26. Yan M, Zhang Z, Wang L, Huang H, Wang J, Zhu C, et al. Cross-talk of Three Molecular Subtypes of Telomere Maintenance Defines Clinical Characteristics and Tumor Microenvironment in Gastric Cancer. *Journal of Cancer*. 2024;15(10):3227-41.
27. Barthel FP, Wei W, Tang M, Martinez-Ledesma E, Hu X, Amin SB, et al. Systematic analysis of telomere length and somatic alterations in 31 cancer types. *Nature genetics*. 2017;49(3):349-57.
28. Zou JJ, Chu SD, Bao QF, Zhang YY. Telomere maintenance genes-derived prognosis signature characterizes immune landscape and predicts prognosis of head and neck squamous cell carcinoma. *Medicine*. 2023;102(31):e34586.
29. Patiyl S, Dhall A, Raghava GPS. Prediction of risk-associated genes and high-risk liver cancer patients from their mutation profile: benchmarking of mutation calling techniques. *Biology methods & protocols*. 2022;7(1):bpac012.
30. Mayakonda A, Lin DC, Assenov Y, Plass C, Koeffler HP. Maftools: efficient and comprehensive analysis of somatic variants in cancer. *Genome research*. 2018;28(11):1747-56.
31. Zheng S, Wang X, Fu Y, Li B, Xu J, Wang H, et al. Targeted next-generation sequencing for cancer-associated gene mutation and copy number detection in 206 patients with non-small-cell lung cancer. *Bioengineered*. 2021;12(1):791-802.
32. Li J, Xie L, Xie Y, Wang F. Bregmannian consensus clustering for cancer subtypes analysis. *Computer Methods and Programs in Biomedicine*. 2020;189:105337.
33. Storey JD, Tibshirani R. Statistical significance for genomewide studies. *Proceedings of the National Academy of Sciences*. 2003;100(16):9440-5.
34. Yu G, Wang L-G, Han Y, He Q-Y. clusterProfiler: an R package for comparing biological themes among

gene clusters. *Omics: A Journal of Integrative Biology*. 2012;16(5):284-7.

35. Xia S, Tao H, Su S, Chen X, Ma L, Li J, et al. DNA Methylation Variation Is Identified in Monozygotic Twins Discordant for Congenital Heart Diseases. *Congenital Heart Disease*. 2024;19(2):247-56.
36. Li Q, Chu Y, Yao Y, Song Q. A Treg-related riskscore model may improve the prognosis evaluation of colorectal cancer. *The Journal of Gene Medicine*. 2024;26(2):e3668.
37. Therneau TM, Lumley T. Package 'survival'. R: Get the Top Words and Documents in Each Topic. 2015;128(10):28-33.
38. Blanche P, Dartigues JF, Jacqmin-Gadda H. Estimating and comparing time-dependent areas under receiver operating characteristic curves for censored event times with competing risks. *Statistics in Medicine*. 2013;32(30):5381-97.
39. Harrell Jr FE, Harrell Jr MFE, Hmisc D. Package 'rms'. Vanderbilt University. 2017;229(Q8).
40. Becht E, Giraldo NA, Lacroix L, Buttard B, Elarouci N, Petitprez F, et al. Estimating the population abundance of tissue-infiltrating immune and stromal cell populations using gene expression. *Genome Biology*. 2016;17(1):218.
41. Zhang X, Jin M, Yao X, Liu J, Yang Y, Huang J, et al. Upregulation of LncRNA WT1-AS Inhibits Tumor Growth and Promotes Autophagy in Gastric Cancer via Suppression of PI3K/Akt/mTOR Pathway. *Current Molecular Pharmacology*. 2024;17.
42. Amuthalakshmi S, Sindhuja S, Nalini CN. A Review on PCR and POC-PCR - A Boon in the Diagnosis of COVID-19. *Current Pharmaceutical Analysis*. 2022;18(8):745-64.
43. Geeleher P, Cox N, Huang RS. pRRophetic: an R package for prediction of clinical chemotherapeutic response from tumor gene expression levels. *Plos One*. 2014;9(9):e107468.
44. Shen W, Song Z, Zhong X, Huang M, Shen D, Gao P, et al. Sangerbox: a comprehensive, interaction-friendly clinical bioinformatics analysis platform. *Imeta*. 2022;1(3):e36.
45. Song ZG, Yu JB, Wang MM, Shen WT, Wang CC, Lu TY, et al. CHDTEPDB: Transcriptome Expression Profile Database and Interactive Analysis Platform for Congenital Heart Disease. *Congenital Heart Disease*. 2023;18(6):693--701.
46. Zhang L, Li D, Du F, Huang H, Yuan C, Fu J, et al. A panel of differentially methylated regions enable prognosis prediction for colorectal cancer. *Genomics*. 2021;113(5):3285-93.
47. Iranmanesh H, Majd A, Nazemalhosseini Mojarad E, Zali MR, Hashemi M. Investigating the Relationship between the Expression Level of Membrane-Bound Mucin (MUC12) and Clinicopathological Characterization of Colorectal Cancer. *Archives of Advances in Biosciences*. 2021;12(1):31-6.
48. Hedrick CC, Malanchi I. Neutrophils in cancer: heterogeneous and multifaceted. *Nature Reviews Immunology*. 2022;22(3):173-87.
49. Hu J, Yu A, Othmane B, Qiu D, Li H, Li C, et al. Siglec15 shapes a non-inflamed tumor microenvironment and predicts the molecular subtype in bladder cancer. *Theranostics*. 2021;11(7):3089-108.
50. Tomasova K, Kroupa M, Forsti A, Vodicka P, Vodickova L. Telomere maintenance in interplay with DNA repair in pathogenesis and treatment of colorectal cancer. *Mutagenesis*. 2020;35(3):261-71.
51. Ma SZ, Zhu XM, Xin C, Cao F, Xu MN, Han XL, et al. RCN3 Expression Indicates Prognosis in Colorectal Cancers. *Oncologie*. 2022;24(4):823--33.
52. Louzon M, Zahn S, Capelli N, Massemin S, Coeurdassier M, Pauget B, et al. Impact of ageing and soil contaminants on telomere length in the land snail. *Ecotoxicology and Environmental Safety*. 2020;201:110766.
53. Hambleton P, Barbieri M-A. A hypothesis for a novel role of RIN1-the modulation of telomerase function by the MAPK signaling pathway. *BioCell*. 2020;44(4):525--34.

54. Huang Z, Zhang Z, Zhou C, Liu L, Huang C. Epithelial–mesenchymal transition: The history, regulatory mechanism, and cancer therapeutic opportunities. *MedComm*. 2022;3(2):e144.
55. Suzuki T, Conant A, Curow C, Alexander A, Ioffe Y, Untch JJ. Role of epithelial-mesenchymal transition factor SNAIL and its targets in ovarian cancer aggressiveness. *Journal of Cancer Metastasis and Treatment*. 2023;9.
56. Tran HD, Luitel K, Kim M, Zhang K, Longmore GD, Tran DD. Transient SNAIL1 Expression Is Necessary for Metastatic Competence in Breast Cancer. *Cancer Research*. 2014;74(21):6330-40.
57. Fang J, Ding Z. SNAIL is a prognostic biomarker and correlated with immune infiltrates in gastrointestinal cancers. *Aging*. 2020;12(17):17167-208.
58. Qing F, Xue J, Sui L, Xiao Q, Xie T, Chen Y, et al. Intestinal epithelial SNAIL promotes the occurrence of colorectal cancer by enhancing EMT and Wnt/ β -catenin signaling. *Medical oncology (Northwood, London, England)*. 2023;41(1):34.
59. Galindo-Pumariño C, Collado M, Castillo ME, Barquín J, Romio E, Larriba MJ, et al. SNAIL-expressing fibroblasts and derived-extracellular matrix as mediators of drug resistance in colorectal cancer patients. *Toxicology and Applied Pharmacology*. 2022;450:116171.
60. Molparia B, Oliveira G, Wagner JL, Spencer EG, Torkamani A. A feasibility study of colorectal cancer diagnosis via circulating tumor DNA derived CNV detection. *Plos One*. 2018;13(5):e0196826.
61. Liu K, Zheng M, Lu R, Du J, Zhao Q, Li Z, et al. The role of CDC25C in cell cycle regulation and clinical cancer therapy: a systematic review. *Cancer Cell International*. 2020;20(1):213.
62. Korbecki J, Bosiacki M, Barczak K, Łagocka R, Brodowska A, Chlubek D, et al. Involvement in Tumorigenesis and Clinical Significance of CXCL1 in Reproductive Cancers: Breast Cancer, Cervical Cancer, Endometrial Cancer, Ovarian Cancer and Prostate Cancer. *International Journal of Molecular Sciences*. 2023;24(8):7262.
63. Sun NH, Zhao X. Therapeutic implications of FABP4 in cancer: an emerging target to tackle cancer. *Frontiers in Pharmacology*. 2022;13:948610.
64. Chen HP, Chen SY, Chen C, Li AF, Wei ZX. Leucine zipper downregulated in cancer 1 may serve as a favorable prognostic biomarker by influencing proliferation, colony formation, cell cycle, apoptosis, and migration ability in hepatocellular carcinoma. *Frontiers in Genetics*. 2022;13:900951.
65. Li H, Liu J, Liu WH, Zheng L, Chen JH. Investigation of potential prognostic biomarkers for colorectal cancer. *Archives of Medical Science*. 2023.
66. Pavai DR, Di Virgilio TG, Skipworth RJ, Gallagher IJ. The emerging role of intelectin-1 in cancer. *Frontiers in Oncology*. 2022;12:767859.
67. Iranmanesh H, Majd A, Mojarad EN, Zali MR, Hashemi M. Investigating the Relationship Between the Expression Level of Mucin Gene Cluster (MUC2, MUC5A, and MUC5B) and Clinicopathological Characterization of Colorectal Cancer. *Galen medical journal*. 2021;10:e2030.
68. Williams SJ, McGuckin MA, Gotley DC, Eyre HJ, Sutherland GR, Antalis TM. Two novel mucin genes down-regulated in colorectal cancer identified by differential display. *Cancer Res*. 1999;59(16):4083-9.
69. Cox KE, Liu S, Lwin TM, Hoffman RM, Batra SK, Bouvet M. The Mucin Family of Proteins: Candidates as Potential Biomarkers for Colon Cancer. *Cancers (Basel)*. 2023;15(5).
70. Pothuraju R, Chaudhary S, Rachagani S, Kaur S, Roy HK, Bouvet M, et al. Mucins, gut microbiota, and postbiotics role in colorectal cancer. *Gut microbes*. 2021;13(1):1974795.
71. Tiwari A, Trivedi R, Lin S-Y. Tumor microenvironment: barrier or opportunity towards effective cancer therapy. *Journal of Biomedical Science*. 2022;29(1):83.
72. De Visser KE, Joyce JA. The evolving tumor microenvironment: From cancer initiation to metastatic

outgrowth. *Cancer Cell International*. 2023;41(3):374-403.

73. Folkman J. Role of angiogenesis in tumor growth and metastasis: Elsevier; 2002. 15-8 p.

74. Plikus MV, Wang X, Sinha S, Forte E, Thompson SM, Herzog EL, et al. Fibroblasts: Origins, definitions, and functions in health and disease. *Cell Division*. 2021;184(15):3852-72.

EARLY ACCESS

TABLES AND FIGURES WITH LEGENDS

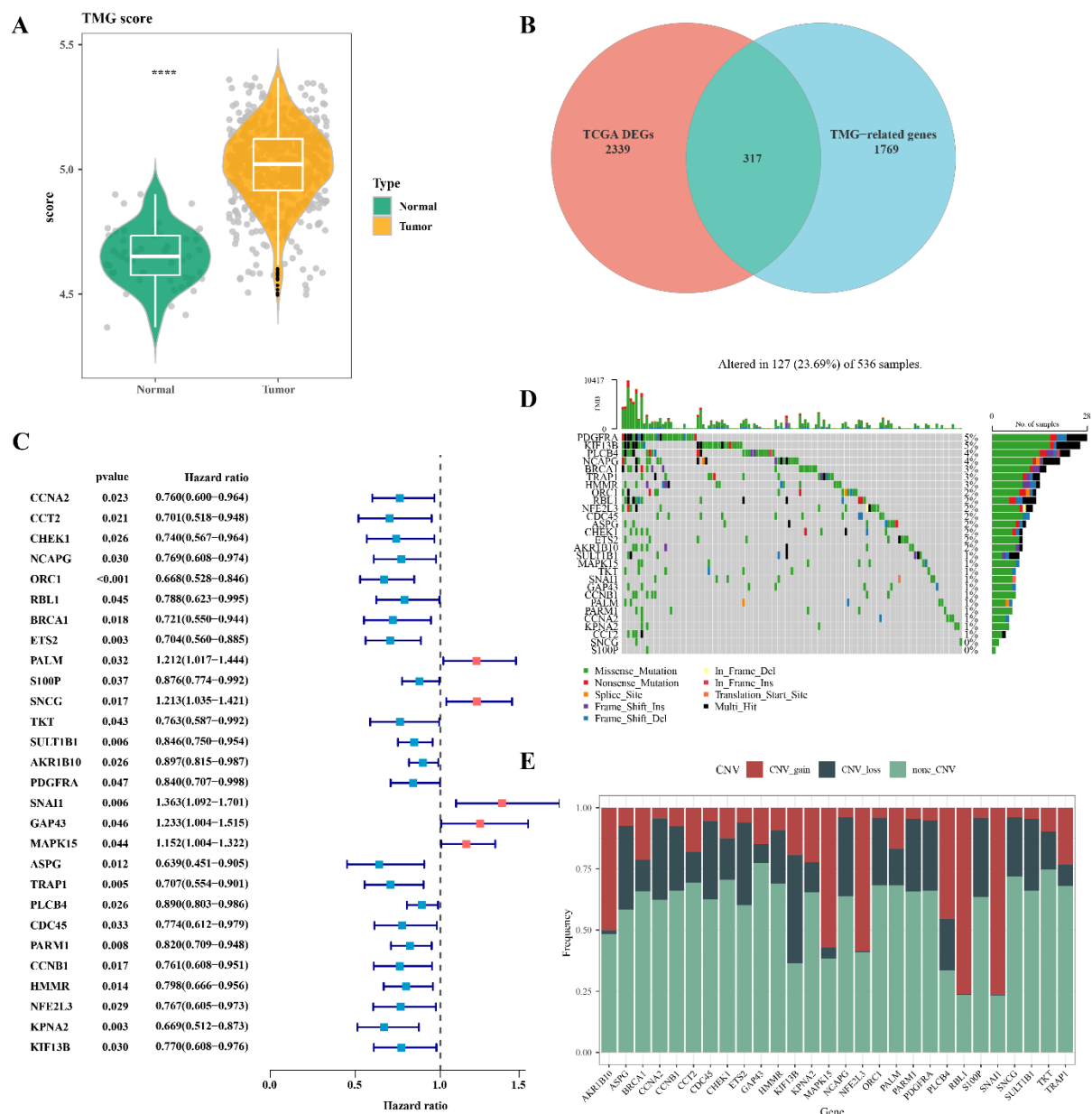


Figure 1. Analysis of the genomic landscape of TMGs in CRC.

(A) The expression of MG scores in CRC and non-cancerous adjacent control samples. (B) The differential genes of tumor tissue and adjacent tissue were intersected with TMG. (C) 28 TMGs were closely linked to CRC prognosis. (D) Mutation status of TMGs in CRC. (E) CNVs of TMGs in CRC.

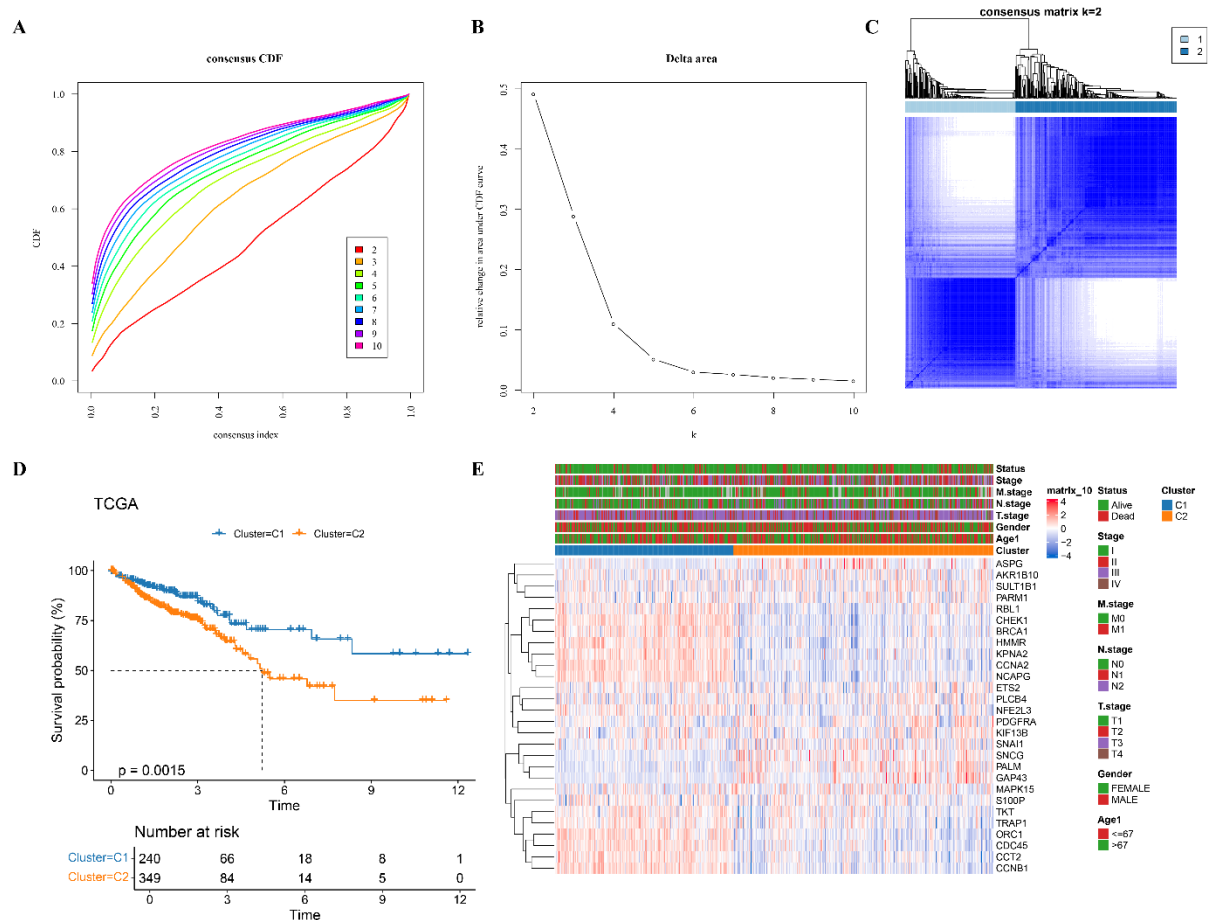
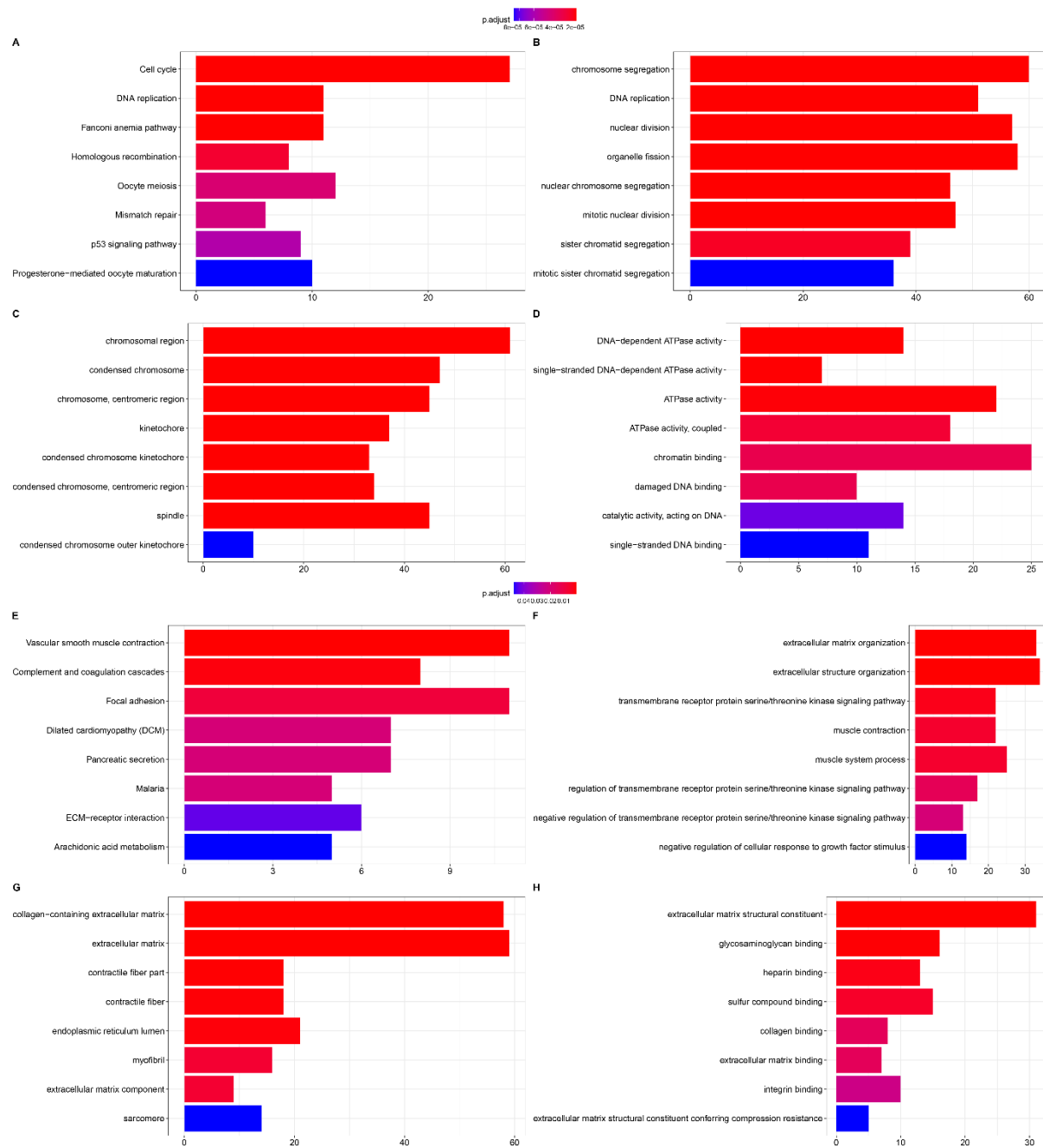


Figure 2. Classification and prognostic differences of TCGA-CRC samples.

(A) CDF curve was plotted for the TCGA-CRC cohort samples. (B) CDF delta area curve was plotted for the TCGA-CRC cohort samples. (C) At consensus k=2, heatmap of sample clustering in the TCGA-CRC cohort was generated. (D) KM curve displaying the relationship between OS and two subtypes in the TCGA-CRC cohort. (E) Heat maps of clinical features (status, stage, M.stage, N.stage, T.stage, age, and gender) and expression between subtypes in the TCGA-CRC cohort.



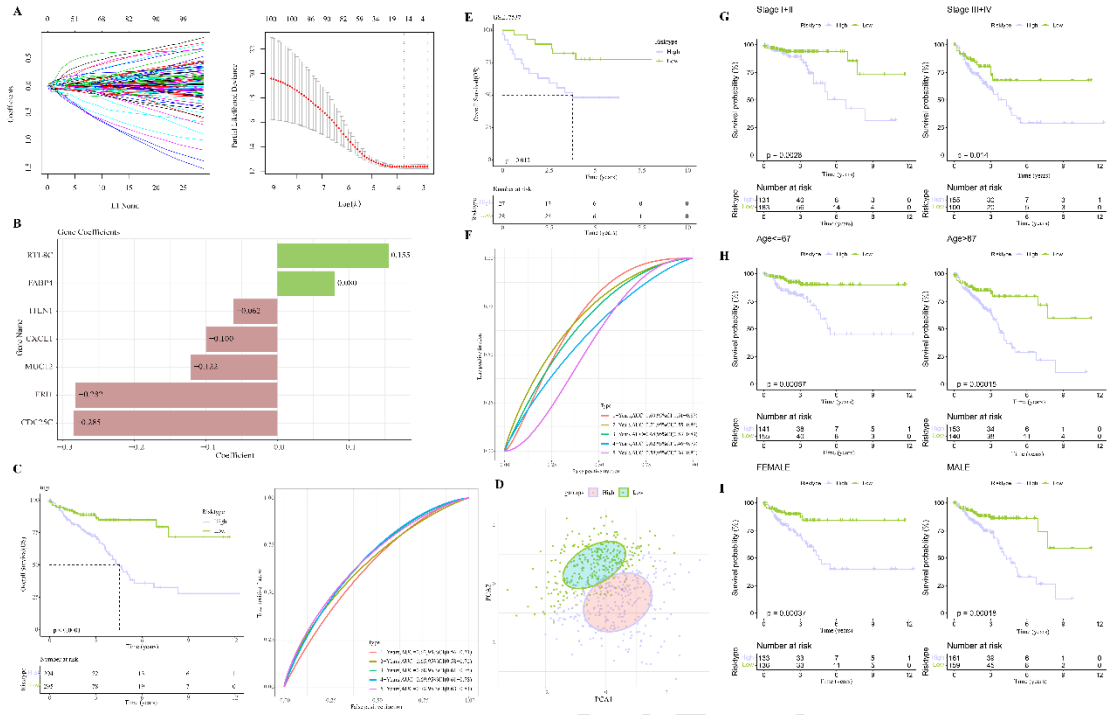
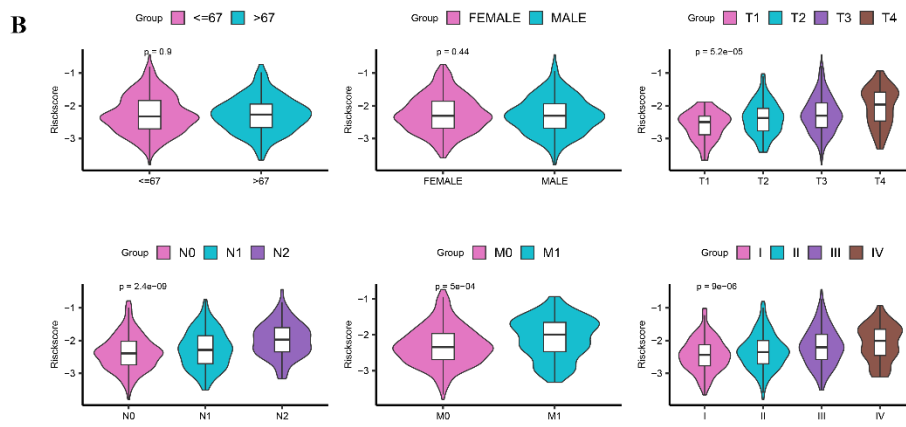
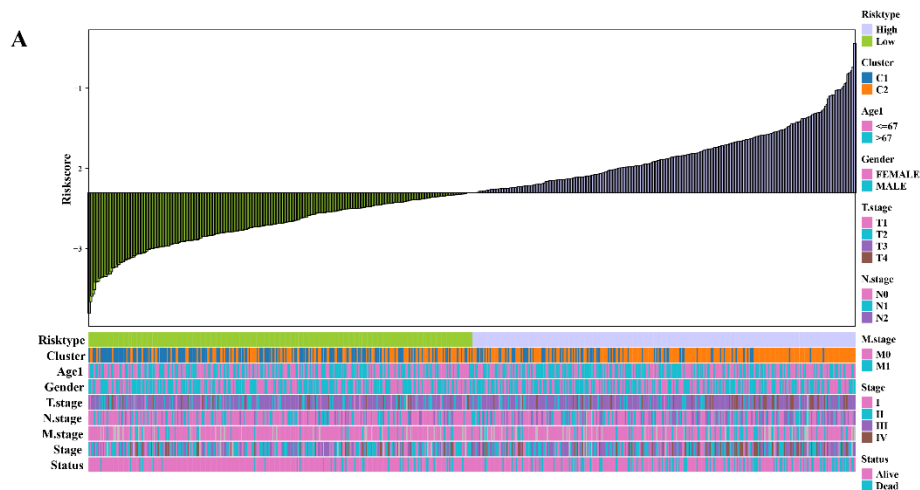


Figure 4. Development of TMGs-based risk model and verification.

(A) LASSO Cox regression analysis was performed to analyze the DEGs linked to CRC prognosis in the TCGA-CRC training cohort. (B) Risk coefficients of key genes in the TCGA-CRC training cohort. (C) KM survival curve and ROC curve for 1-, 3- and 5-year prognostic prediction for TCGA-CRC training cohort. (D) PCA comparing low- and high-risk groups within the TCGA-CRC training cohort. (E-F) KM survival curves and ROC curves for the model based on the GEO testing dataset. (G-I) Prognosis differences between the two risk groups across different tumor stages (G), ages (H), and genders (I).



C

| Names | p.value | Hazard Ratio(95% CI) |
|-----------|---------|----------------------|
| Age | <0.001 | 1.03(1.01,1.05) |
| Gender | 0.738 | 1.06(0.74,1.53) |
| T.stage | 0.006 | 2.5(1.3,4.79) |
| N.stage | <0.001 | 2.76(1.89,4.04) |
| M.stage | <0.001 | 4.55(3.04,6.81) |
| Stage | <0.001 | 3.21(2.15,4.82) |
| RiskScore | <0.001 | 2.72(1.99,3.71) |

D

| Names | p.value | Hazard Ratio(95% CI) |
|-----------|---------|----------------------|
| Age | <0.001 | 1.04(1.02,1.06) |
| T.stage | 0.117 | 1.98(0.84,4.64) |
| N.stage | 0.077 | 0.42(0.16,1.1) |
| M.stage | <0.001 | 2.83(1.73,4.61) |
| Stage | 0.007 | 4.58(1.53,13.72) |
| RiskScore | <0.001 | 2.13(1.5,3.03) |

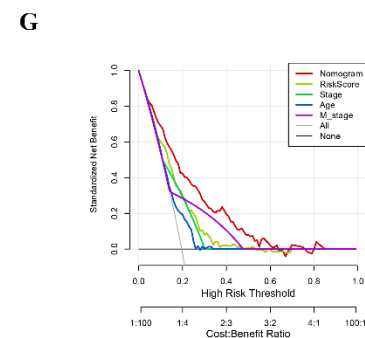
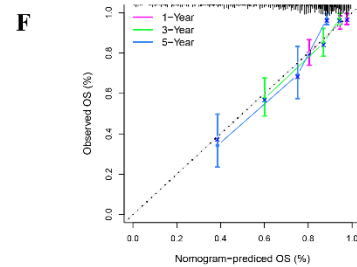
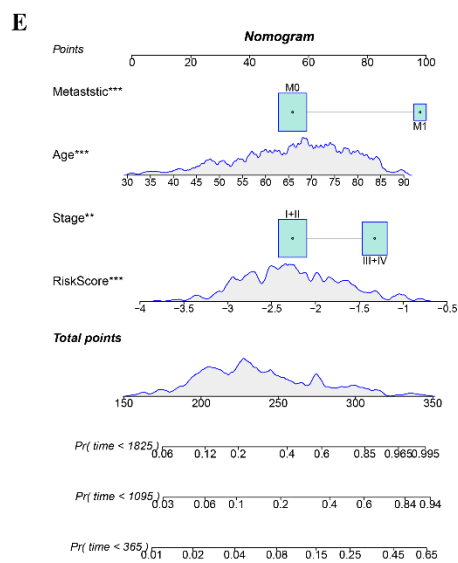


Figure 5. Development of a nomogram to assess CRC prognosis.

(A) Relationship between RiskScore and clinical characteristics (M.stage, N.stage, T.stage, stage, status, age, and gender). (B) Violin plots illustrating the distribution of clinical characteristics (status, M.stage, N.stage, T.stage, stage, age and gender) between low-risk and high-risk groups. (C-D) Univariate and multivariate COX regression analyses were performed to determine the effect of RiskScore and clinical characteristics (status, stage, M.stage, N.stage, T.stage, age and gender). (E) Nomogram to predict the 1-, 3-, and 5-year OS of CRC patients. (F) Calibration curve used to verify established nomogram. (G) DCA of nomogram. * $P < 0.05$; ** $P < 0.01$; *** $P < 0.001$.

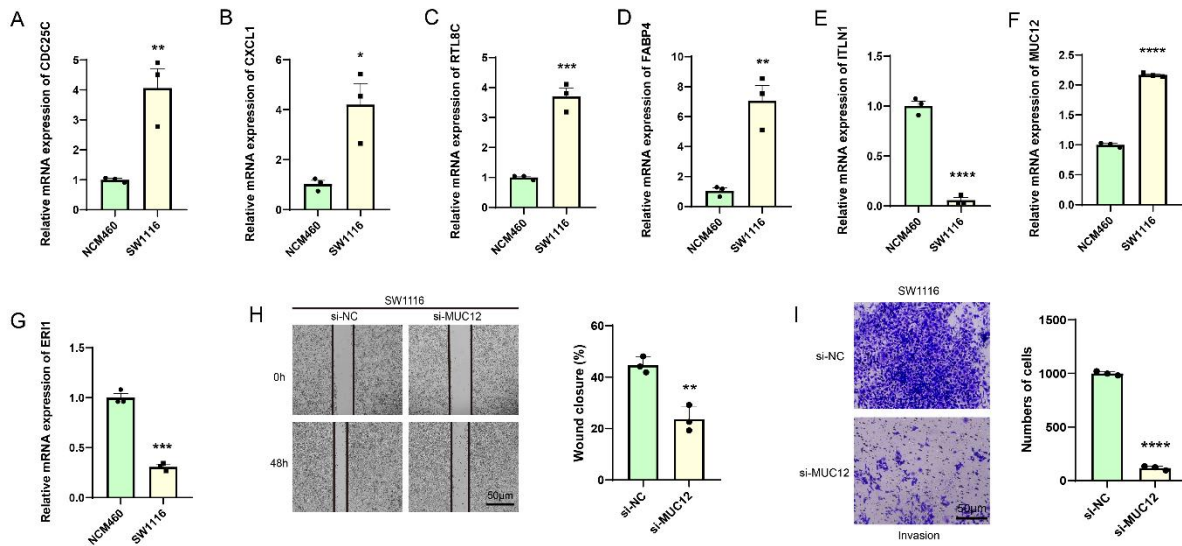


Figure 6. In-vitro validation using CRC cells

(A-G) Quantified expression levels of 7 biomarkers CDC25C (A), CXCL1 (B), RTL8C (C), FABP4 (D), ITLN1 (E), MUC12 (F) and ERI1 (G) in CRC cells SW1116 and human normal colonic epithelial cells NCM460 via qRT-PCR. (H) Effects of MUC12 silencing on the migration of CRC cells SW1116 tested via wound healing assay. (I) Effects of MUC12 silencing on the invasion of CRC cells SW1116 tested via transwell assay. All the data from three independent experimental sets were shown as mean \pm standard deviation. * $P < 0.05$; ** $P < 0.01$; *** $P < 0.001$; **** $P < 0.0001$.

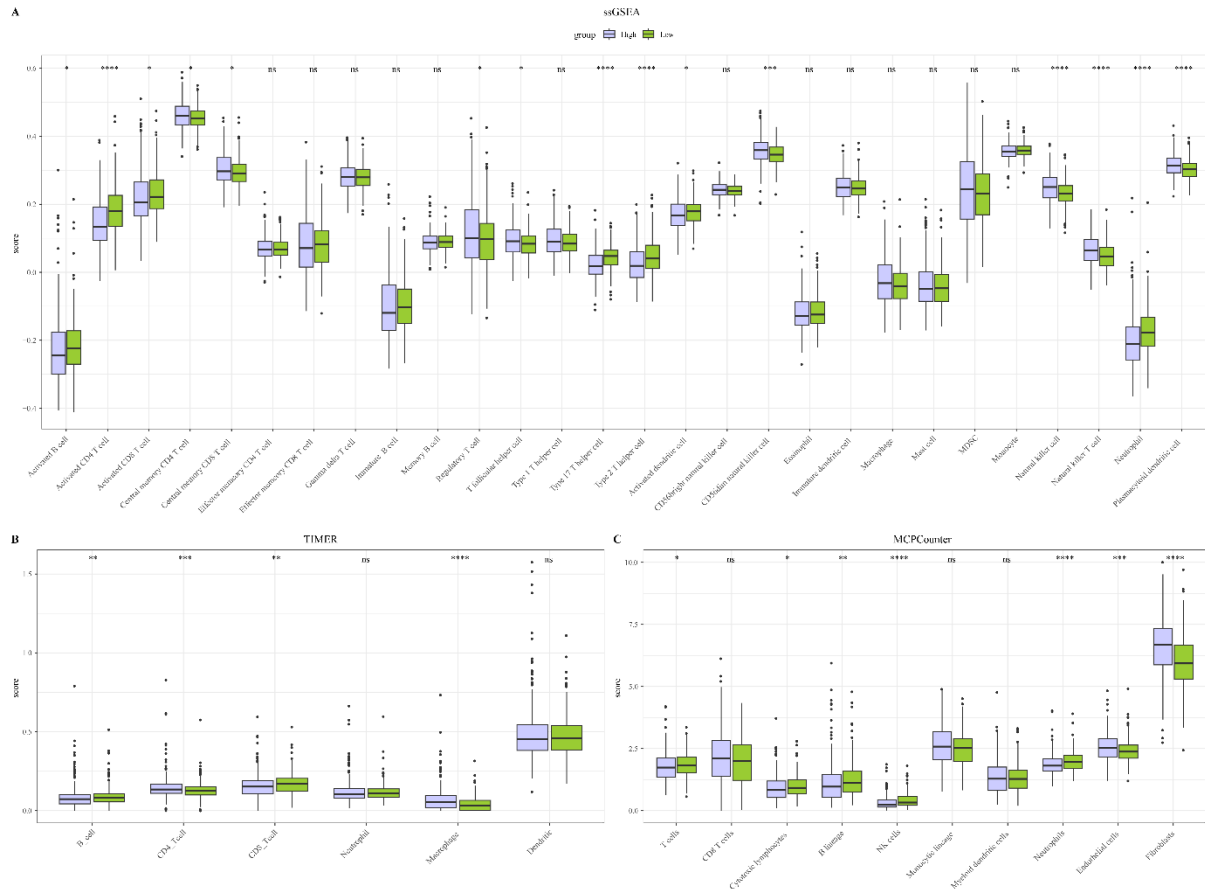


Figure 7. Analysis of differences in immune infiltration levels between high- and low-risk groups

(A-C) The method of (A) ssGSEA, (B)TIMER and (C)MCPcounter was used to calculate the immune infiltration levels of the two risk groups, respectively.

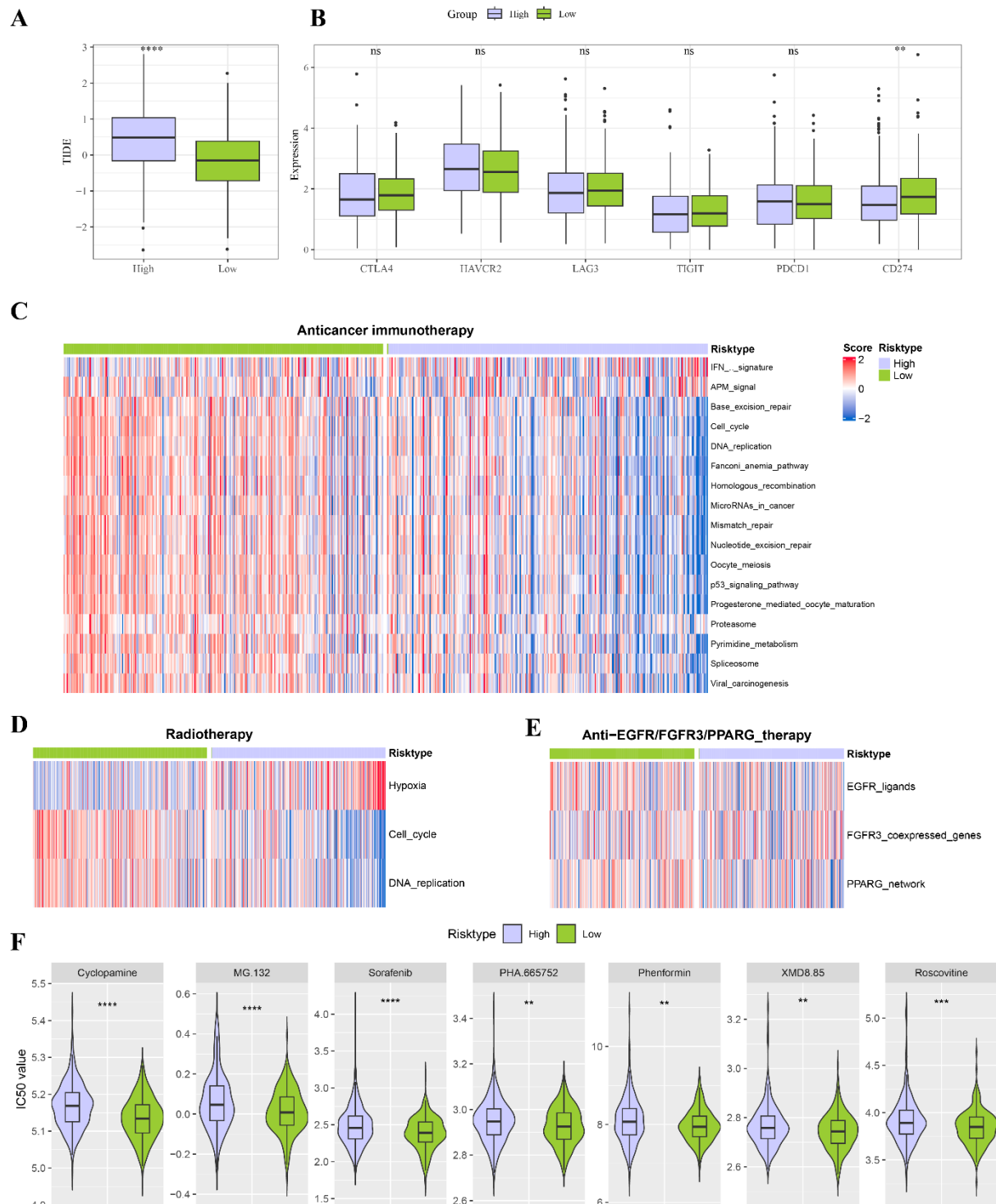


Figure 8. Immunotherapy and drug sensitivity studies between high and low risk groups.

(A) Differences in TIDE scores between high and low risk groups. (B) Variations in common immune checkpoint expressions between high and low risk groups. (C-E) Results of differences in response to (C) Anticancer immunotherapy, (D) Radiotherapy, (E) Anti-EGFR/FGFR3/PPARG_therapy between high and low risk groups. (F) Differences in

drug sensitivity of Cyclopamine, MG-132, Sorafenib, PHA.665752, Phenformin, XMD8.85 and Roscovitine were observed between high-risk and low-risk groups.

SUPPLEMENTAL DATA

Table S1. Primer sequences used in this study.

| Gene | Accession | Primers (5'-3') | |
|---------------|------------|----------------------------------|----------------------------|
| | No. | Forward | Reverse |
| <i>CDC25C</i> | NM_001790 | AAGGCGGCTACAGAGAC TTCTT | AGAGTTGGCTGGCTTGT GAGA |
| <i>CXCL1</i> | NM_001511 | TGCTGCTCCTGCTCCTGG TA | GCTTTCCGCCCATCTTG AGTG |
| <i>RTL8C</i> | NM_001078 | AAGCGAGGAGCAGCGAT 171 GGA | TGTGAGGCGGGTGATGA GGAA |
| <i>FABP4</i> | NM_001442 | TGCAGCTTCCTTCTCACC TTGA | TGACGCATTCCACCACC AGTT |
| <i>ITLN1</i> | NM_017625 | AACGCCTTGTGTGCTGG AATGA | ATCTCACGGCTGCTGCT GTAAC |
| <i>MUC12</i> | NM_0011644 | CCTCAACTCACACGACG 62 CCTTC | TGCTGCTGTAGACGGTG GTAGA |
| <i>ERII</i> | NM_153332 | ATCCTCTTGCCTCAGCCT CCT | TTCAAGACCAGCCTGAC CAACA |
| <i>GAPDH</i> | NM_002046 | GTCTCCTCTGACTTCAAC AGCG | ACCACCCTGTTGCTGTA GCCAA |

RELATED ARTICLES

[Pan-Cancer Analysis of HPRT1 Prognostic significance and immunological role of HPRT1 in human cancers](#)

Biomol Biomed, 2023

[PD-L1 testing by immunohistochemistry in immuno-oncology](#)

Semir Vranic, Biomol Biomed, 2023

[Systemic analysis of the expression and prognostic significance of USP31 in endometrial cancer](#)

Yuzhen Huang, BJBMS, 2022

EARLY ACCESS